

# Multi-Frame Blind Image Deconvolution through Split Frequency - Phase Recovery

Adam Gauci<sup>a</sup>, John Abela<sup>a</sup>, Ernest Cachia<sup>a</sup>, Michael Hirsch<sup>b</sup>, Kristian ZarbAdami<sup>c</sup>

<sup>a</sup>Faculty of ICT, University of Malta

<sup>b</sup>Dept. Empirical Inference, MPI for Intelligent Systems

<sup>c</sup>Dept. of Astrophysics, Oxford University

## ABSTRACT

Accurate information extraction from images can only be realised if the data is blur free and contains no artificial artefacts. In astronomical images, apart from hardware limitations, biases are introduced by phenomena beyond control such as atmospheric turbulence. The induced blur function does vary in both time and space depending on the astronomical “seeing” conditions as well as the wavelengths being recorded. Multi-frame blind image deconvolution attempts to recover a sharp latent image from an image sequence of blurry and noisy observations without knowledge of the blur applied to each image within the recorded sequence. Finding a solution to this inverse problem that estimates the original scene from convolved data is a heavily ill-posed problem. In this paper we describe a novel multi-frame blind deconvolution algorithm, that performs image restoration by recovering the frequency and phase information of the latent sharp image in two separate steps. For every given image in the sequence a point-spread function (PSF) is estimated that allows iterative refinement of our latent sharp image estimate. The datasets generated for testing purposes assume Moffat or complex Kolmogorov blur kernels. The results from our implemented prototype are promising and encourage further research.

**Keywords:** Multi-frame blind deconvolution, Manhattan norm minimisation, Euclidian norm minimisation.

## 1. INTRODUCTION

The study of images in scientific fields such as remote sensing, medical imaging and astronomy comes natural not only because pictures simulate one of the main sensory elements of humans, but also because they allow for the visualisation of wavelengths to which the eyes are not sensitive. However, accurate information extraction from images can only be realised if the data is known to be noise free, blur free and that it contains no artefacts.

Image deconvolution attempts to recover the true intensity values from measured ones. Having a robust and accurate algorithm is very important especially for telescopes such as the Square Kilometre Array (SKA) through which sensitive investigations including gravitational lensing research and the detection of faint sources, are to be made. Despite the non-uniqueness and noise sensitivity, a lot of research in deconvolution methods have been proposed by major scientific communities including those focusing on computer vision, optics and astronomy.

Most of the existing deblurring techniques assume the filter to be known and attempt recovery by using this information. While the point-spread function (PSF) of the instrument may be resolved with very high accuracy, scientific images such as those found in astrophysics or medicine contain random spatially-varying factors that change on millisecond scales. For instance, in optical astronomy, the PSF can be considered constant over an isoplanatic patch for 5 to 15ms across regions between 10 and 20cm [1]. Longer exposure times will cause the high frequency components to average out while shorter recording times will not be enough to record all information. In such cases, the true blur kernel cannot be accurately known and blind deconvolution methods have to be used.

The blind deconvolution problem is a heavily ill-posed inverse problem. Finding a solution that removes the spreading to obtain the original image from the recorded intensities, is challenging. Due to the nature of the problem, a unique solution does not exist. This work improves on previous work [1] and investigates the improvements gained when a number of blurred frames that capture the same source are used to estimate the original scene. A hybrid norm minimisation technique that performs optimisation in pixel and Fourier spaces to separately recover the frequency and phase information, is proposed. For every presented image, the PSF is first estimated and used to deblur the presented

frame. With subsequent iterates, more accurate blur filters are estimated and the global image converges towards the true scene.

## 2. BLURRED IMAGE DATA

Images do not always represent the true intensities being irradiated by the sources. The output quality of an imaging instrument depends on its degradation function which acts as a filter and distorts the captured product. A recorded image  $I$  at time  $t$  corresponds to the actual observed intensities  $O$  as described by Equation (1)

$$\begin{aligned} I_t(x, y) &= (O \otimes P_t)(x, y) + s(x, y) \\ &= \sum_{-\infty}^{\infty} \sum_{-\infty}^{\infty} O(x - u, y - v) P_t(u, v) + s(x, y) \end{aligned} \quad (1)$$

Where  $P$  is the PSF,  $s$  is the noise (which is often assumed to be Gaussian and uncorrelated with the image) and  $\otimes$  denotes the two dimensional convolution operator.  $P$  forms part of the simplex of all kernels with positive elements that add up to one. The value of the grid cell at position  $(x, y)$  in image  $I$  results from the weighting of the real intensities according to the filter defined by  $P$ .

From a given blurred image and the corresponding PSF, the non-blurred scene can be estimated by minimising the Euclidian norm ( $\ell_2$ ) as shown in Equation (2) with respect to  $O$ . Similarly, if the target scene is known, the PSF can be estimated by minimising this same equation with respect to  $P_t$ . In both cases, a positive prior can be employed and solutions can be obtained up to an error threshold ( $\varepsilon$ ) depending on the noise level. Convolution can also be represented as multiplication in the frequency domain ( $\mathcal{F}$ ). This allows recovery of  $O$  and  $P_t$  through the minimisation of the Manhattan norm ( $\ell_1$ ) as demonstrated by Equation (3).

$$\min \|I_t - (O \otimes P_t)\|_2^2 \leq \varepsilon \quad (2)$$

$$\min \|O\|_1 \text{ such that } \|I_t - \mathcal{F}^{-1}[\mathcal{F}(O)\mathcal{F}(P_t)]\|_2^2 \leq \varepsilon \quad (3)$$

Non-trivial convolution kernels that simulate the blur effects of the atmosphere and the ionosphere can be generated through Kolmogorov models that average different Gaussian amplitudes and phase independent Fourier modes. This work considers such filters to shift and blur the image content. Solutions for Equation (2) can be obtained through the use of Non-Negative Least Square (NNLS) techniques. Recent research in Machine Learning has led to significant advances in the field of Compressed Sensing (CS) which focuses on recovering the important signal coefficients from an incomplete set of measurements. A number of fast, robust and reliable algorithms that can come up with a solution for Equation (3) have been proposed [2].

Radio telescopes make use of array configurations to synthesize large apertures through the distribution of small antennas over large areas to record frequency samples. As the Earth rotates and the sources traverse the sky, the visibilities measured by the interferometer will form an elliptical path in Fourier space. The number of measured frequencies is much less than the amount specified by the Nyquist-Shannon theorem of twice the signal's bandwidth so the sampled Fourier coverage is incomplete. A direct conversion from Fourier to image space will result in the objects to appear blurred. In [3]-[7], the use of CS to enhance radio interferometric images was already investigated. For instance, the Sparsity Averaging Reweighted Analysis (SARA) algorithm assumes average signal sparsity and makes use of CS techniques to reconstruct the original data [8], [9]. Although this and other similar techniques manage to converge towards a very good reconstruction, the frequency mask needs to be accurately known. Moreover, blurring is achieved by multiplying the mask with the magnitude of the Fourier representation of the image. As demonstrated in Fig. 1, realistic PSFs have a strong phase component.

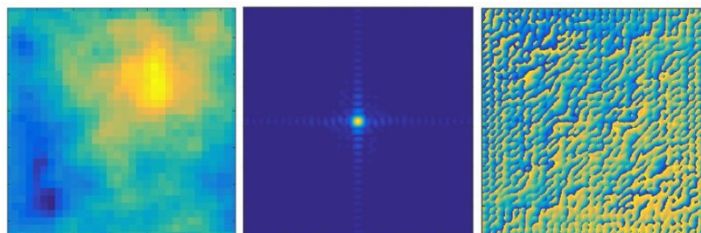


Figure 1. Kolmogorov PSF in image space (left), frequency coefficients (middle) and corresponding phase shifts (left).

### 3. DEBLURRING THROUGH FOURIER DECOMPOSITION

In this work, a hybrid approach that makes use of  $\ell_1$  and  $\ell_2$  minimisation for the deblurring of images is investigated. As shown in Fig. 2, the frequency and phase information of the unknown PSFs as well as of the global estimate are recovered separately. The solution vectors are projected onto a complex space and the pixel representation is obtained through an inverse Fourier Transform.

#### 3.1 Frequency and Phase Recovery

The frequency encoding of astronomical images can be represented by a sparse vector. Although few coefficients might be large, most of the entries will be very small or null. Hence, CS methods can be applied to obtain a solution for Equation (3). Solvers such as the Primal-Dual Interior Point Method and the Total Variation minimiser which are implemented in the  $\ell_1$ -MAGIC toolbox [10] as well as the Compressive Sampling Matching Pursuit method [11] were tested. However, the Spectral Projected-Gradient L1 (SPGL1) algorithm [12] proved to provide the best results.

The phase vector that encodes the shift of each component, is bound between  $\pm\pi$ . This information is not sparse so the same approach adopted for frequency recovery cannot be used. In the implemented technique, phases are extracted from the solution obtained by solving Equation (2) using the Limited memory Broyden Fletcher Goldfarb Shanno algorithm with bound constraints (L-BFGS-B) is used [13].

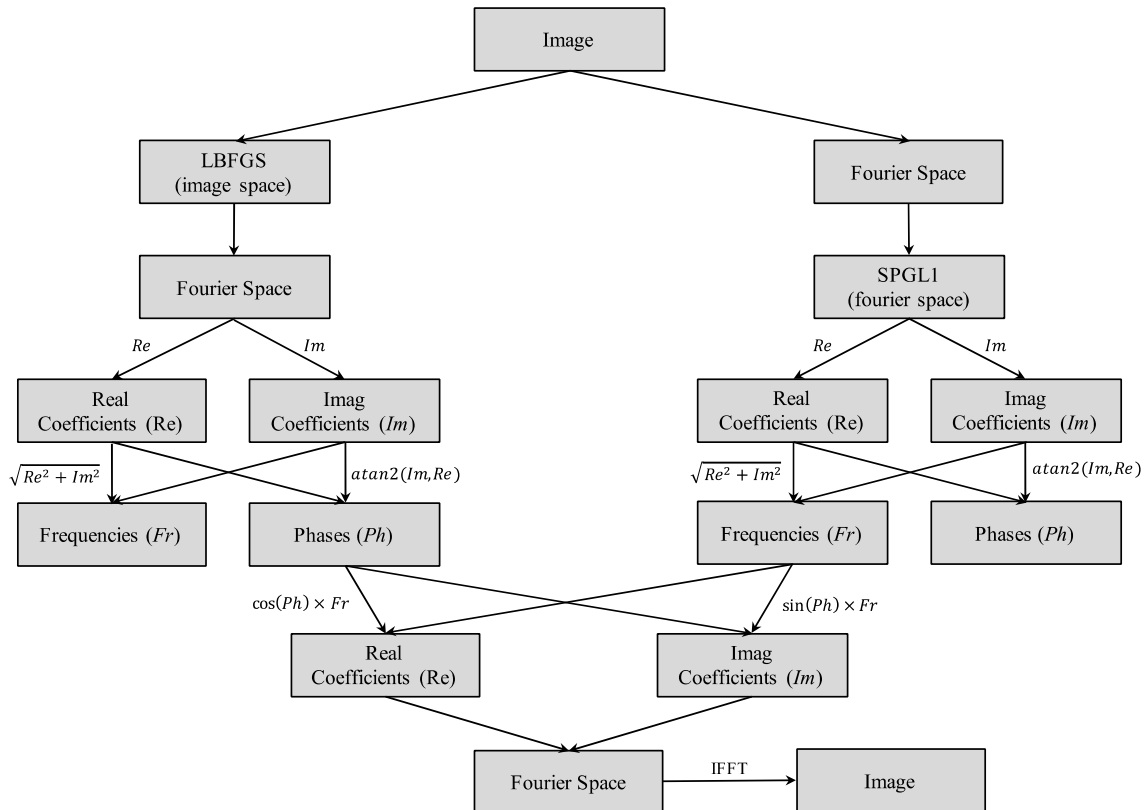


Figure 2. Decomposition and recovery processes for frequency and phase spaces recovery.

#### 3.2 Iterative Blind Deconvolution

In the previous section, our novel framework to recover an image from its blurred version and the corresponding PSF was proposed. The same mathematical model can also be used to obtain the PSF when the original and blurred frames are known. However, in order for the technique to be useful in real-life scenarios, recovery must be possible by making use of the captured blurred frames only. The proposed approach involves using a number of images to extract information and iteratively constructs the unblurred scene.

In the first iterate, the PSF ( $P_1$ ) is assumed to be a delta function and the input image ( $I_1$ ) is taken to be the global estimate ( $O_1$ ). In the second step, the new input image ( $I_2$ ) together with the current global estimate ( $O_1$ ) are used to compute the PSF ( $P_2$ ). The next step involves deblurring of the input image by using the available global estimate and the identified PSF ( $P_2$ ). The global estimate is updated with the new deblurred version and the process is repeated until no further input data is available. For the general case, in every iterate  $t$ , for input image  $I_t$  and with the previous global estimate given by  $O_{t-1}$ , the frequency and phase information of the PSF ( $P_t$ ) are first estimated up to a tolerance of  $\varepsilon_t$ . The same method is then applied over  $I_t$  and  $P_t$  to obtain  $O_t$ . Since the first few iterates will only have rough versions of the PSF and of the target scene, the error threshold is gradually reduced according to an inverse sigmoid function.

## 4. RESULTS

A prototype of the proposed method was implemented and tested on a number of simulated yet realistic images. Datasets were generated by filtering an image with 50 different PSFs. Shifted Moffat profiles and Kolmogorov kernels were used. The results of the first few and last iterates when processing an image of the OCNR5 satellite, are shown in Fig. 3. As evident from the postcards on the top row, a lot of details are lost in the individual blurred frames. However, the algorithm manages to accurately recover most of the information with a high degree of accuracy.

Another set of results obtained after processing blurred images of the M31 galaxy, are presented in Fig. 4. Even though closely located bright sources bleed into each other within the dirty images, these are gradually recovered in the global estimate.

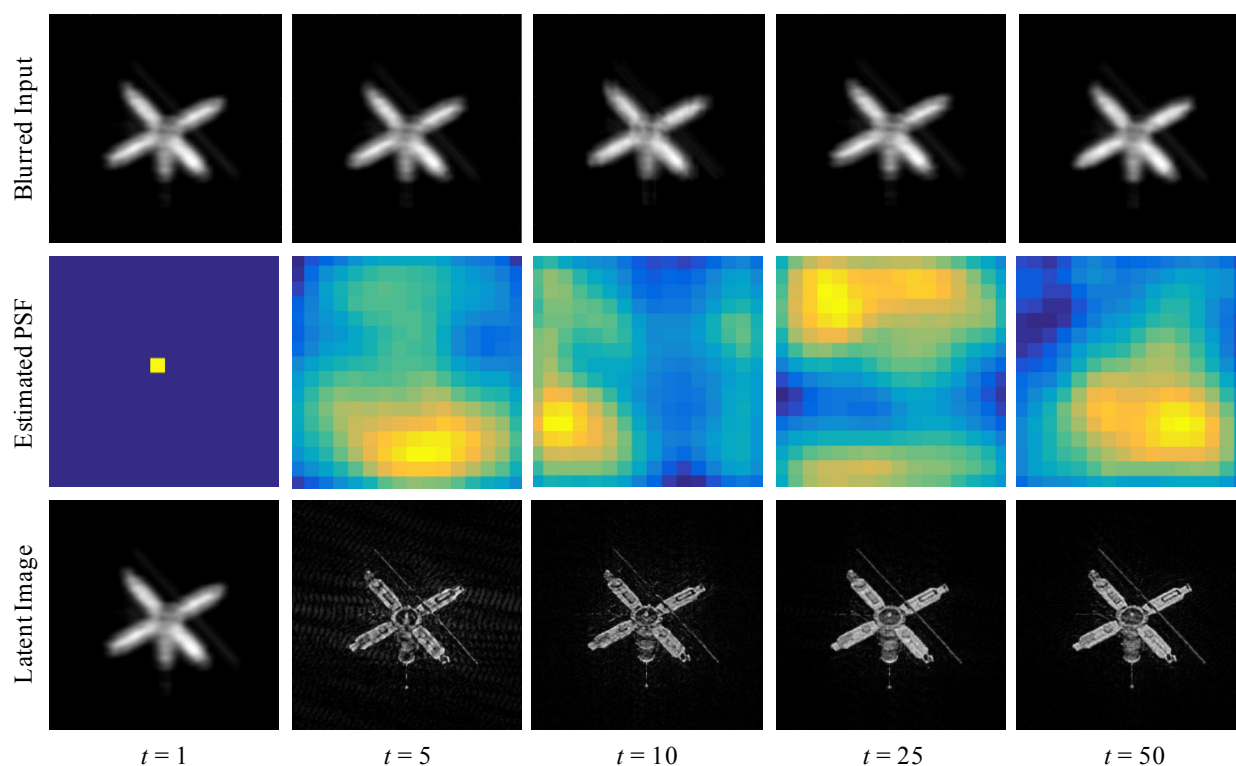


Figure 3. Blurred input images of the OCNR5 satellite (top row), estimated PSFs (middle row) and recovered estimate (bottom row) for selected iterates

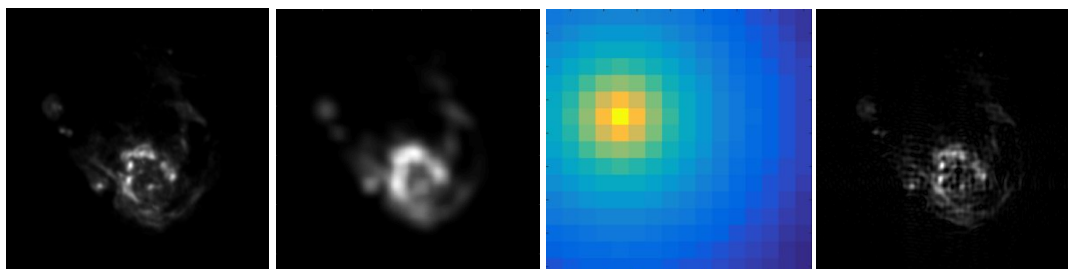


Figure 4. Original image of the M31 galaxy, typical blurred input image, corresponding Moffat PSF and the recovered estimate (left to right).

## 5. CONCLUSION

The main goal of this research was to investigate the advantages gained when combining  $\ell_1$  and  $\ell_2$  minimisation for blind deconvolution. Our presented method allows for the reconstruction of the original scene from a number of frames that were blurred by different unknown filters. A prototype of the proposed technique was implemented and tested on simulated images. The preliminary results are promising and encourage further research. The quality metrics computed between the original and deblurred images prove that very good reconstructions were achieved.

Frequency information of astronomical signals is sparse and hence recovery through the minimisation of the Manhattan norm is possible. On the other hand, phase encoding is chaotic and completely changes with small shifts in the centre of gravity of the PSF. Although the presented method proves to provide an accurate estimate for the frequencies components, more work is required to further optimise the corresponding shift information. While the features and structures within the images are recovered, phase errors cause ringing in the computed global estimate.

Research to further improve on the proposed method for phase recovery is ongoing. Fusion techniques to combine the images generated in the last few iterates, are also being investigated. Such an approach is expected to provide a monotonic error decay despite the level of blurriness in the input image. Improvements gained in the final recovery through image alignment prior to deblurring, is also being examined.

## REFERENCES

- [1] Hirsch, M., Harmeling, S., Sra, S. and Schölkopf, B., Online multi-frame blind deconvolution with super-resolution and saturation correction, *Astronomy and Astrophysics*, 531:A9, (2011).
- [2] Baraniuk, R., Davenport, M., Duarte, M. and Hegde, C., *An Introduction to Compressive Sensing*, Connexions e-textbook, (2011).
- [3] Suksmono, A. B., Deconvolution of VLBI images based on compressive sensing, *International Conference on Electrical Engineering and Informatics*, 1:110-116, (2009).
- [4] Li, F., Cornwell, T. J. and DeHoog, F., *The Applications of Compressive Sensing to Radio Astronomy*, Lecture Notes in Computer Science, Springer, 6221:352–359, (2010).
- [5] McEwen, J. D. and Wiaux, Y., Compressed sensing for radio interferometric imaging: review and future, *International Conference On Image Processing (ICIP)*, 1313-1316, (2011).
- [6] Garsden, H., Girard, J. N., Starck, J. L., et al., LOFAR Sparse Image Reconstruction, *arXiv:1406.7242*, (2014).
- [7] Carrillo, R. E., McEwen, J. D. and Wiaux, Y., PURIFY: a new approach to radio-interferometric imaging, *Monthly Notices of the Royal Astronomical Society (MNRAS)*, 439 (4):3591-3604, (2014).
- [8] Carrillo, R. E., McEwen, J. D., Van De Ville, D., Thiran, J. P. and Wiaux, Y., Sparsity averaging for compressive imaging, *Computing Research Repository*, 1208.2330, (2012).
- [9] Carrillo, R. E., McEwen, J. D. and Wiaux, Y., Sparsity averaging reweighted analysis (SARA): a novel algorithm for radio-interferometric imaging, *Monthly Notices of the Royal Astronomical Society (MNRAS)*, 426:1223–1234, (2012).
- [10] Boyd, D. and Vandenberghe, L., *Convex Optimization*, Cambridge University Press, New York, NY, USA, (2004).

- [11] Needell, D. and Tropp, J. A., CoSaMP: Iterative Signal Recovery From Incomplete and Inaccurate Samples, *Communications of the ACM*, 53(12):93-100, (2010).
- [12] Van den Berg, E. and Friedlander, M. P., Probing the pareto frontier for basis pursuit solutions, *SIAM Journal on Scientific Computing*, 31(2): 890–912, (2008).
- [13] Byrd, R. H., Lu, P., Nocedal, J. and Zhu, C., A limited memory algorithm for bound constrained optimization, *SIAM Journal on Scientific Computing*, 16(5):1190–1208, (1995).